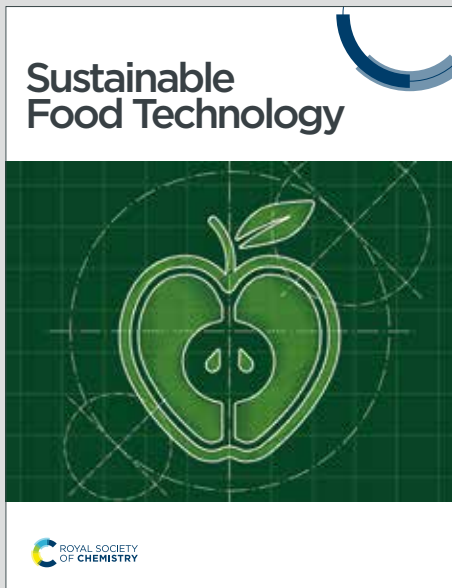


# Sustainable Food Technology

Accepted Manuscript

This article can be cited before page numbers have been issued, to do this please use: N. Rana, R. Satwalia and A. Saneja, *Sustainable Food Technol.*, 2025, DOI: 10.1039/D5FB00838G.



This is an Accepted Manuscript, which has been through the Royal Society of Chemistry peer review process and has been accepted for publication.

Accepted Manuscripts are published online shortly after acceptance, before technical editing, formatting and proof reading. Using this free service, authors can make their results available to the community, in citable form, before we publish the edited article. We will replace this Accepted Manuscript with the edited and formatted Advance Article as soon as it is available.

You can find more information about Accepted Manuscripts in the [Information for Authors](#).

Please note that technical editing may introduce minor changes to the text and/or graphics, which may alter content. The journal's standard [Terms & Conditions](#) and the [Ethical guidelines](#) still apply. In no event shall the Royal Society of Chemistry be held responsible for any errors or omissions in this Accepted Manuscript or any consequences arising from the use of any information it contains.

**Sustainability Spotlight:**

This study advances sustainable packaging by creating biodegradable starch/PVA–PEG copolymer films infused with green tea extract (TE). By replacing petroleum-based plastics with renewable, compostable materials, the films reduce plastic pollution and dependence on fossil resources. Their natural antioxidant and antibacterial properties extend food shelf life, decreasing food waste. This innovation directly supports UN Sustainable Development Goals 12 (Responsible Consumption and Production), 13 (Climate Action), and 14 (Life Below Water) by promoting circular material use, mitigating environmental impact, and protecting ecosystems from plastic contamination. Overall, the work exemplifies a holistic approach to developing eco-friendly packaging solutions for a more sustainable future.



# Development of Multifunctional and Sustainable Starch/Polyvinyl Alcohol–Polyethylene Glycol Copolymer Films Reinforced with Green Tea Extract for Food Packaging

Neha Rana<sup>a,b</sup>, Ruchika<sup>a,b</sup>, Ankit Saneja<sup>a,b\*</sup>

<sup>a</sup>Formulation Laboratory, Dietetics and Nutrition Technology Division, CSIR-Institute of Himalayan Bioresource Technology, Palampur-176061, Himachal Pradesh, India

<sup>b</sup>Academy of Scientific and Innovative Research (AcSIR), Ghaziabad – 201002, India

8

9

10

11

12

13

14

15

16

## \*Corresponding Author

Dr. Ankit Saneja

Senior Scientist

Dietetics and Nutrition Technology Division,

CSIR – Institute of Himalayan Bioresource Technology,

Palampur, 176061

Himachal Pradesh, India

E-mail: [ankit.saneja@csir.res.in](mailto:ankit.saneja@csir.res.in); [ankitsaneja.ihbt@gmail.com](mailto:ankitsaneja.ihbt@gmail.com)

Tel: 91-1894-233339, Ext: 485

26



27 **Abstract**

28 This study explores a sustainable alternative to conventional plastic packaging by  
29 developing biodegradable films from starch, polyvinyl alcohol–polyethylene glycol  
30 (PVA-PEG) copolymer and green tea extract (TE) as functional additive. The  
31 incorporation of TE at 0.5 % w/v demonstrated to significantly enhance tensile strength  
32 ( $4.7 \pm 0.3$  MPa) and water contact angle ( $70.7 \pm 0.3^\circ$ ) in comparison to blank STKB  
33 film. The developed films also demonstrated significant improvement in barrier  
34 attributes of the film including, UV-shielding (100%), water vapour and oxygen  
35 transmission. Further, the films were analysed *via* several techniques, including  
36 Scanning Electron Microscopy (SEM), 3D optical profilometry, Fourier Transform  
37 Infrared Spectroscopy (FTIR), X-ray Diffraction (XRD) and Thermogravimetric  
38 Analysis (TGA). The results demonstrated that incorporating TE improved the  
39 structure, intermolecular interactions and thermal stability of the film. The DPPH assay  
40 and cytocompatibility (95 %) in L929 fibroblast confirmed the strong antioxidant and  
41 biocompatibility of the developed film. The incorporation of TE enhanced the  
42 antibacterial potential of the films, with significant inhibition of *Escherichia coli* and  
43 *Staphylococcus aureus*. The preservation application of developed films on fresh cut  
44 apple cubes demonstrated reduced browning index, weight loss and pH indicated  
45 better preservation compared to the blank film. Finally, the biodegradability of the film  
46 was assessed by soil burial tests demonstrated residual area ( $99.35 \pm 0.64$ ) within 10  
47 days. These results highlight the potential of ST/PVA-PEG/TE films as eco-friendly,  
48 functional packaging materials to improve food shelf life while ensuring safety and  
49 sustainability.

50

51 **Keywords:** Biodegradable films, green tea extract, Starch/PVA-PEG, Antioxidant  
52 properties, Antibacterial activity, Fresh-cut apple preservation

53

54

55

56

57



## 58 1. Introduction

View Article Online  
DOI: 10.1039/D5FB00838G

59 Increasing concerns about plastic pollution have intensified the quest for sustainable  
60 packaging solutions for food preservation while being environmentally friendly<sup>1, 2</sup>.  
61 Traditional petroleum-based plastics remain in the environment for decades, collecting  
62 in landfills and waterways, which has sparked interest in renewable and biodegradable  
63 options that align with circular-economy principles. Biopolymer films are particularly  
64 noteworthy as they can provide food protection while minimizing long-term  
65 environmental impact when properly disposed off<sup>3, 4</sup>. Starch, an abundant and cost-  
66 effective polysaccharide, is a primary focus for biodegradable food packaging due to  
67 its effective film-forming capacity and natural compostability. Starch-based films are  
68 widely used in different food applications due to their desirable features, such as high  
69 transparency, good sensory qualities, and excellent gas barrier properties<sup>5, 6</sup>.  
70 However, their broader application in food packaging is hindered by drawbacks like  
71 low water resistance and weak mechanical strength. A promising approach to enhance  
72 their performance is to develop blend films by incorporating starch polymers with other  
73 compatible polymers<sup>7-9</sup>.

74 By blending starch with other polymers, the films may gain enhanced strength and  
75 integrity, while the addition of polyethylene glycol (PEG) serves as a plasticizer,  
76 improving flexibility and allowing for better control over water interactions<sup>7, 10, 11</sup>. To  
77 further enhance functionality beyond simple physical protection, researchers are  
78 increasingly integrating natural bioactive into biopolymer matrices. Green tea extract  
79 (TE), rich in catechin polyphenols, is recognized for its antioxidant and antimicrobial  
80 properties, making it effective in combating oxidation and inhibiting foodborne  
81 pathogens<sup>12, 13</sup>. The incorporation of TE into biodegradable films has shown to boost  
82 radical-scavenging activity and provide antibacterial benefits essential for extending  
83 shelf life and ensuring food safety<sup>13-16</sup>.

84 Therefore, this study focuses on developing a starch/PVA-PEG copolymer film that  
85 incorporates TE, aiming to combine biodegradability with inherent antioxidant and  
86 antibacterial functions. In this study, we have blended PVA-PEG copolymer with starch  
87 and TE. The main objective was to present a sustainable alternative to conventional  
88 plastics that also actively contributes to maintaining food quality. Further, instead of  
89 utilizing an external plasticizer, PVA-PEG copolymer was utilized, which has intrinsic



90 plasticizing properties. This approach provides the advantage of eliminating extra  
91 optimization step needed for external plasticizer to avoid leaching phenomenon in the  
92 films. Further, PVA-PEG copolymer is well known for its excellent film forming ability  
93 and commonly utilized in pharmaceutical industries <sup>17</sup>. Beyond functional  
94 improvements, the selection of bioactive ingredients and polymer blends considered  
95 biocompatibility and safety for food contact, which is crucial for packaging. A thorough  
96 characterization investigated based on mechanical and surface properties was carried  
97 to analyse the influences of TE on the structure and properties of the films. The  
98 morphology and surface topography was analysed using scanning electron  
99 microscopy (SEM) and 3D optical profilometry. The chemical interactions and  
100 molecular ordering were studied through Fourier-transform infrared spectroscopy  
101 (FTIR) and X-ray diffraction (XRD) to understand hydrogen bonding and crystallinity  
102 modifications within the starch/PVA-PEG/TE matrix. Additionally, thermogravimetric  
103 analysis (TGA) was utilized to determine thermal stability and degradation behaviour  
104 under heat, key attributes concerning processing and usability. The functional  
105 performance was evaluated through standard antioxidant assay, such as DPPH  
106 radical scavenging, to measure oxidative protection capabilities along with migration  
107 studies. The cytocompatibility of the developed films were assessed through fibroblast  
108 (L929) cell viability tests to confirm the safety. Further, the antibacterial activity was  
109 also conducted against common foodborne pathogens, including *Escherichia coli* and  
110 *Staphylococcus aureus*, using colony forming unit methodology. To demonstrate  
111 practical applicability, the films was utilized for packaging of fresh-cut apples, which  
112 are susceptible to enzymatic browning, moisture loss, weight loss, and pH of the fruit.

## 113 2. Experimental section

### 114 2.1. Materials

115 Potato starch (ST) was purchased from Central Drug House Limited (India). Kollicoat®  
116 IR (PVA-PEG copolymer) and DPPH were obtained from Sigma-Aldrich. All other  
117 reagents used were of analytical grade. L929 fibroblast cells were obtained from  
118 NCCS, Pune, India. The two bacterial strains [*Escherichia coli* (MTCC 43) and  
119 *Staphylococcus aureus* (MTCC 96)] were procured from MTCC, India.

120



121 **Preparation of green tea extract (TE)**View Article Online  
DOI: 10.1039/D5FB00838G

122 The green tea was collected from the institutional tea processing facility. The green  
123 tea extract (TE) was prepared by adding 5 g of green tea to 500 mL of distilled water  
124 and heat at 80 °C for 20 min with continuous stirring. The obtained solution was then  
125 filtered to remove any residues. The filtrate was condensed using rotatory evaporator  
126 (RV10, IKA, Germany) at 40 °C followed by freeze-drying <sup>13, 18</sup>. The extract was  
127 removed with help of spatula and grinded to obtain the green tea extract powder. The  
128 total phenolic content (TPC) of TE was estimated *via* Folin-ciocalteu method and  
129 expressed as gallic acid amount in mg/gm dry weight of the TE <sup>19</sup>. The TPC of all the  
130 samples was assessed in three replicates, and the average value was reported.

131 **2.2. Preparation of Starch/PVA-PEG/Green tea extract films (STKTE films)**

132 The different film forming solutions were prepared by blending ST and PVA-PEG co-  
133 polymer (KIR) as the primary film base using solvent casting method <sup>18</sup>. Briefly, Starch  
134 6% (w/v) and PVA-PEG co-polymer 11 % (w/v) were dissolved in distilled water with  
135 continuous stirring at 60°C, in two separate beakers. Once completely dissolve, the  
136 solutions were combined in 1:1 ratio (v/v) and stirred for other 30 min. The tea extract  
137 (TE) at different concentrations (0.25, 0.5 and 1 % w/v) was added to primary film base  
138 to get three different films: (i) ST/KIR/TE 0.25 % (w/v) films (STKTE 0.25%); (ii)  
139 ST/KIR/TE 0.5 % (w/v) films (STKTE 0.5%); (iii) ST/KIR/TE 1 % (w/v) films (STKTE  
140 1%). The obtained homogeneous solutions were casted on a flat surface with a digital  
141 adjustable applicator (VJ Instruments, India) to get films of uniform thickness. The films  
142 were dried at room temperature and stored till further use. The blank film STKB was  
143 also prepared, constituting of Starch and PVA-PEG co-polymer only. The thickness of  
144 films was determined using a digital micrometer and expressed in mm (millimetres).

145 **2.3. Optimization of STKTE films**146 **2.4.1. Film mechanical attributes**

147 The tensile strength (TS) and elongation at break (EAB) of developed film samples  
148 were measured using a “tensile tester (SSIC-TTM-50 kgf-SC, SISCO, India)”. Prior to  
149 testing, the film samples were cut into 100 mm\*20 mm strips and tested at a specific  
150 force rate.



151 **2.4.2. Water Contact Angle (WCA)**

152 The WCA was measured using a “DMe-211 Plus contact angle meter (Kyowa, Japan)”  
153 following the sessile drop method<sup>20</sup>. Before experiment, the film samples (20 × 20 mm)  
154 were placed flat on the sample stage, and a droplet (2 ± 0.1 µL) of distilled water was  
155 deposited carefully on the film sample. The contact angle was recorded immediately  
156 after deposition followed by capturing of images and analyzed using FAMAS software.

157 **2.4. Solid state characterization and barrier property analysis of STKB and  
158 STKTE 0.5% Films**159 **2.4.1. Scanning Electron Microscopy (SEM)**

160 The surface morphologies of STKB and STKTE 0.5% films were examined by  
161 “Scanning Electron microscope (SEM, Hitachi S-3400 N, 15 kV)”. The film samples  
162 (10 × 10 mm) were fixed on metal stubs with help of adhesive carbon tape and sprayed  
163 with gold to ensure conductivity and clear imaging<sup>20, 21</sup>.

164 **2.4.2. 3D Optical profilometry**

165 The topology and roughness of the STKB and STKTE 0.5% film samples were  
166 examined using an “optical profilometer (Contour GT-K, Bruker AXS, USA)” operated  
167 in confocal mode<sup>22</sup>.

168 **2.4.3. Colour and UV-shielding analysis**

169 The UV–Visible spectrophotometer “(GENESYS™ 180, Thermo Scientific, USA)”, was  
170 used to determine the transmittance of the STKB and STKTE 0.5% film samples. The  
171 transmission spectrum was recorded in the range between 200-800 nm<sup>23</sup>. The Color  
172 parameters L\* (lightness), a\* (red/green), b\* (Yellow/blue) and ΔE (Total color difference)  
173 of the films were evaluated using a color Reader (CR6, China).

174 **2.4.4. Fourier Transform Infrared Spectroscopy (ATR-FTIR)**

175 The possible molecular interaction between ST, PVA-PEG (KIR), TE, STKB and  
176 STKTE 0.5% films was studied by using an “infrared spectrophotometer (Agilent  
177 Technologies, USA)”. The spectra were recorded between wavenumber ranging from  
178 500–4000 cm<sup>-1</sup><sup>24</sup>.



179 **2.4.5. X-ray Diffraction (XRD)**View Article Online  
DOI: 10.1039/D5FB00838G

180 The crystallinity of ST, PVA-PEG (KIR), TE, STKB and STKTE 0.5% films was  
181 examined with a “X-ray diffractometer (Malvern Panalytical diffractometer, UK)”. The  
182 diffraction patterns were recorded over a 2θ range of 5° to 40°<sup>5</sup>.

183 **2.4.6. Thermogravimetric Analysis (TGA)**

184

185 The thermal properties of ST, PVA-PEG, TE and STKB and STKTE 0.5% films were  
186 analyzed by a “Thermogravimetric analyzer, TA Instruments Discovery Series  
187 TGA5500 (Waters, USA)”. Concisely, small amount of sample was placed into pans  
188 and heated from 25°C to 550°C at a rate of 20°C/min under nitrogen flow and % weight  
189 was recorded<sup>25</sup>.

190

191 **2.4.7. Opacity, Moisture Content, and Barrier properties of STKB and STKTE  
192 0.5% films**

193 The opacity of STKB and STKTE 0.5% films samples were analysed by recording  
194 absorbance using an “UV-visible spectrophotometer (GENESYS™ 180 UV-  
195 spectrophotometer, Thermo Scientific, USA)” at a specific wavelength of 500 nm<sup>26</sup>.  
196 The opacity was deduced using following equation:

197 Opacity of films =  $A_{500} * X$  .....equation 1

198 where  $A_{500}$  is absorbance of film samples and X is thickness of film (mm).

199 The % moisture content of the STKB and STKTE 0.5% films was evaluated via  
200 “UniBloc moisture analyzer (MOC 63u, Shimadzu, Japan)”. The water vapour  
201 permeability (WVP) of the film samples was tested by following ASTM E96 standard  
202 using payne permeability cups (Raj Make, India)<sup>27</sup>. Initially, the test cups were filled  
203 with 3 mL of distilled water, sealed with films and placed in vacuum desiccator for 24  
204 h. The change in weight (g) of the test cups was recorded and WVP was calculated.

205 Water vapor permeability of films =  $\frac{\Delta W \times X}{A \times t \times \Delta P}$  ...equation

206 2



207 Where,  $\Delta W$  represents the test cup weight change (g),  $x$  is film thickness (mm), A  
 208 corresponds to the film area ( $m^2$ ),  $t$  is the time period (s), and  $\Delta P$  is the water vapor  
 209 pressure difference (Pa).

210 An indirect method was used to analyse the oxygen transmission across the film<sup>28</sup>.  
 211 Briefly, the centrifuge tubes containing 3 g of deoxidizer (iron powder), were sealed  
 212 with films and placed at 25 °C and weighed after 48 hrs. The oxygen permeability (OP)  
 213 of films was determined using following equation:

214 Oxygen Permeability ( $10^{-6}g.mm.m^{-2}.s^{-1}$ ) =  $(\Delta m \times d) / (A \times t)$  ...equation 3

215 where  $\Delta m$  is the mass change (g) of the tube,  $d$  is the film thickness (mm),  $t$  is the time  
 216 (s) and  $A$  denotes the permeation area ( $m^2$ ).

## 217 2.5. Determination of antioxidant activity of STKB and STKTE 0.5% films

218 The antioxidant activity of the STKB and STKTE 0.5% films was estimated using 2,2-  
 219 diphenyl-1-picrylhydrazyl (DPPH) assay<sup>13, 21</sup>. Briefly, 1 mL of various film  
 220 concentrations (125, 250, 500, 750, and 1000  $\mu$ g/mL) was added to 2 mL of DPPH  
 221 solution, vortexed, and incubated in the dark for 30 min. The absorbance at 517 nm  
 222 was determined using a "UV-spectrophotometer (GENESYS™ 180, Thermo Scientific,  
 223 USA)" and % radical scavenging activity of films were deduced using the equation:

224 % scavenging activity of films =  $\left( \frac{A_0 - A_1}{A_0} \right) * 100\%$  .....equation 4

225 Where,  $A_0$  and  $A_1$  denotes absorbance of the blank DPPH solutions and absorbance  
 226 of solution with film sample, respectively.

## 227 2.6. Migration study of tea extract in STKTE 0.5% films

228 The migration behaviour of the TE incorporated in STKTE 0.5% film, was estimated  
 229 using total immersion method with three different simulants (simulant A-water,  
 230 simulant B- 3 % acetic acid and 95% ethanol)<sup>29</sup>. In short, film samples (1×3 cm) were  
 231 immersed in 5 ml of simulant and incubated in dark at 40°C for a period of 10 days.  
 232 After incubation, the absorbance of the samples at 268 nm was recorded and migrated  
 233 TE content was deduced by calibration curve of TE. Moreover, the antioxidant activity  
 234 of the solution obtained after the migration test was also estimated using DPPH assay.



**235 2.7. Biocompatibility of STKB and STKTE 0.5% films**

View Article Online  
DOI: 10.1039/D5FB00838G

236 The fibroblast murine cells (L929 cells) was utilized to assess the biocompatibility of  
237 STKB and STKTE 0.5% films <sup>21, 30</sup>. Briefly, the L929 cells were seeded and treated  
238 with different film concentrations (5, 25, 50, 75 and 100 µg/mL) for 24 h at 37°C. The  
239 MTT assay was used to assess the effect of films on L929 cells and % cell viability  
240 was calculated using the following equation:

241 % Cell viability of fibroblast cells =  $\left( \frac{\text{Absorbance of sample}}{\text{Absorbance of control}} \right) * 100$  ..... equation 5

242 In addition, the cells were subjected to staining using the “Live/Dead™ Cell Imaging  
243 Kit (Invitrogen, Thermo Fisher Scientific)” after treatment with the films. The images of  
244 fibroblast cells were captured using the “ZOE™ Fluorescent Cell Imager (Bio-Rad)” to  
245 determine live and dead cells <sup>31</sup>.

**246 2.8. Antibacterial assessment of STKB and STKTE 0.5% films**

247 The antibacterial efficacy of STKB and STKTE 0.5% films was assessed against two  
248 bacterial strains *viz.* *E. coli* (gram-negative) and *S. aureus* (gram-positive) <sup>28</sup>. Prior to  
249 experiment, the film samples were sterilized *via* UV light treatment for 30 min. Further,  
250 sterilized film samples (20 mg/mL) were dissolved in 25 mL of liquid medium  
251 inoculated with either *E. coli* (Luria broth) or *S. aureus* (Nutrient broth) and incubated  
252 for 12 h (at 37°C) with continuous agitation. The OD of samples were observed at  
253 specific intervals (1, 2, 4, 6, 8, 10 and 12h) and after incubation the diluted (6-fold)  
254 bacterial suspension (100 µL) was uniformly spread over the sterile agar plates. The  
255 number of colonies were counted with help of Handheld Digital Colony Counter  
256 (HIMEDIA). The bacterial suspension without film sample considered as control. The  
257 number of colonies counted were expressed in CFU/mL by using following equation:

258 Colony Forming units per mL of film samples =  $\frac{(\text{No. of colonies} \times \text{Dilution factor})}{\text{Volume of culture plated}}$  ...equation

259 6

**260 2.9. Application in fresh cut apple preservation**

261 Apple preservation was assessed using STKB and STKTE 0.5% films to estimate their  
262 potential in maintaining shelf life and quality of apple during storage. The fresh apples



263 were procured from local market at Palampur (H.P), washed thoroughly and cut into  
 264 cubed shaped pieces (2×2 cm). The apple cubes were divided into four groups (in  
 265 triplicates with 3 apple cubes in each replicate) *viz.* Group 1: uncovered (control);  
 266 Group 2: covered with conventional polyethylene packaging (PE); Group 3: covered  
 267 with STKB film and Group 4: covered with STKTE 0.5% film. The fresh cut apples were  
 268 stored at room temperature for a period of 5 days. All the groups were analysed during  
 269 storage period for their Weight loss (%), pH and visual appearance<sup>32</sup>. For visual  
 270 appearance, the images were captured at regular time intervals. The % weight loss  
 271 was calculated using equation:

$$272 \text{ Weight loss (\%)} = \left( \frac{W_i - W_d}{W_i} \right) * 100 \quad \dots \dots \text{equation 7}$$

273 Where,  $W_i$  and  $W_d$  is the initial weight and weight at the day of the apple cubes,  
 274 respectively.

275 The color parameters ( $L^*$ ,  $a^*$  and  $b^*$  value) of the apple cubes were measured using  
 276 colorimeter “(CR-6, 3nh Technology, China)”, at different time points during storage.  
 277 The browning index (BI) was evaluated to determine the browning degree of the apple  
 278 cubes during preservation period <sup>33</sup>. The BI of apple cubes was calculated according  
 279 to following equation:

$$280 \text{ BI of fresh cut apple} = \frac{y - 0.31}{0.172} \times 100 \quad \dots \dots \text{equation 8}$$

$$281 \text{ where, } y = \frac{a + 1.75L}{5.645L + a - 3.02b}$$

## 282 2.10. Soil burial test assessment of STKB and STKTE 0.5% films

283 The STKB and STKTE 0.5% film's physical disintegration was estimated by soil burial  
 284 test <sup>34</sup>. Briefly, the film samples STKB and STKTE 0.5% (2× 2 cm) were placed  
 285 between the mesh layers and buried at a depth of 10 cm in the soil. The films were  
 286 regularly monitored and photographed at specific time intervals for a period of 10 days.  
 287 The residual area of the film samples was measured using ImageJ software and  
 288 calculated using following equation:

$$289 \text{ \% residual film area} = \left( \frac{\text{Residual area of the film}}{\text{Initial area of the film}} \right) * 100 \quad \dots \dots \text{equation 9}$$



290

View Article Online  
DOI: 10.1039/D5FB00838G291 **2.11. Statistical analysis**

292 The statistical analysis of the obtained results was performed using GraphPad Prism  
293 10 (GraphPad Software Inc., CA, USA). The t-test and one-way or two-way analysis  
294 of variance (ANOVA), followed by Tukey's post-hoc test was employed to compare  
295 differences between the groups with statistical significance considered at  $p < 0.05$ . All  
296 results were expressed as mean  $\pm$  standard deviation (SD).

297 **3. Results and discussion**298 **3.1. Optimization and selection of tea extract incorporated ST/PVA-PEG  
299 copolymer/TE (STKTE) film**

300 Starch-based packaging films have gained considerable interest as eco-friendly  
301 alternatives to petroleum-based plastics due to their biodegradability, renewability,  
302 and cost-effectiveness. However, films composed solely of starch often face several  
303 limitations, such as high brittleness, inadequate mechanical strength, and significant  
304 hydrophilic tendencies, which lead to increased moisture sensitivity and reduced water  
305 resistance<sup>6, 22, 35-38</sup>. These challenges limit their direct application in food packaging  
306 and other uses that require flexibility, durability, and moisture stability. To overcome  
307 these issues, a PVA-PEG copolymer was integrated into the starch matrix. This  
308 copolymer has inherent plasticizing properties thanks to its flexible ether linkages and  
309 hydroxyl groups, which enhance intermolecular hydrogen bonding and facilitate chain  
310 mobility<sup>22, 39</sup>.

311 Further, TE was incorporated as a functional additive to impart additional active  
312 properties and reinforce the film structure. TE, rich in polyphenolic content ( $458.9 \pm$   
313 0.5 mg GAE/g), can form strong interactions with polymeric chains through hydrogen  
314 bonding and hydrophobic interactions<sup>19, 40-43</sup>. The addition of such extracts impacts  
315 the films mechanical and barrier properties in multifaceted manner. Therefore, the  
316 ST/PVA-PEG copolymer films were optimized based on tensile strength, elongation at  
317 break and water contact angle with varying concentration of tea extract. The TE was  
318 incorporated in three different concentrations (w/v) into the polymeric solution which  
319 resulted in formation of three different types of films viz. STKTE 0.25 %, STKTE 0.5  
320 %, and STKTE 1 % (**Figure 2**).



321 The blank film composed of only Starch and PVA-PEG copolymer demonstrated the  
322 TS of  $2.2 \pm 0.9$  MPa, EAB of  $1.7 \pm 0.5$  % and WCA of  $58.6 \pm 0.6^\circ$ . The addition of TE  
323 in the polymeric matrix impacts the mechanical and water contact angle in a bell-  
324 shaped manner<sup>22, 24, 42</sup>. Specifically, the film with lowest concentration of TE (STKTE  
325 0.25 %) exhibited lowest TS ( $1.03 \pm 0.4$  MPa), EAB ( $2.2 \pm 0.5$  %), and WCA ( $60.9 \pm$   
326  $5.4^\circ$ ). Further, a significant enhancement in the mechanical as well as WCA of film  
327 was observed in film with 0.5% of TE (STKTE 0.5 %) which showed TS of  $4.7 \pm 0.3$   
328 MPa, EAB ( $3.6 \pm 1.5$  %), and WCA ( $70.7 \pm 0.3^\circ$ ), indicating enhanced intermolecular  
329 interaction between TE and film components<sup>22</sup>. However, further increase in TE  
330 amount (STKTE 1 %), the mechanical attributes and WCA decreases, might be due  
331 to saturation and agglomeration. Conclusively, STKTE 0.5 % film demonstrated  
332 enhanced mechanical and WCA parameters, therefore selected for further  
333 experiments.

334 < Insert Figure 2>

### 335 3.2. Characterization of developed ST/PVA-PEG copolymer/TE (STKTE) film

#### 336 3.2.1. Surface and morphological analysis of STKB and STKTE 0.5% film

337 SEM and 3D profilometry analysis was conducted to observe the surface morphology  
338 and microstructural variations before and after incorporation of TE in the film (**Figure**  
339 **3**). The SEM analysis reveals that the morphology shifts from larger, irregular domains  
340 in the pure STKB film to smaller, more uniformly distributed domains in the STKTE  
341 0.5% film, implying improved dispersion or interaction at the microscopic level. Further,  
342 the optical profilometry data demonstrated slight increase in the average peak height  
343 ( $R_{pm}$ :  $6.5 \pm 2.4$   $\mu\text{m}$ ) and  $R_z$  (roughness of film) value ( $37.9 \pm 5.4$   $\mu\text{m}$ ) in STKTE 0.5%  
344 film in comparison to STKB film ( $R_{pm}$ :  $4.3 \pm 1.2$   $\mu\text{m}$  and  $R_z$ :  $35.7 \pm 3.03$   $\mu\text{m}$ ). The  $R_{pm}$   
345 and  $R_z$  values provide essential information on surface roughness, which directly  
346 influences the mechanical integrity, wettability, and overall uniformity of food  
347 packaging films. The lower values of  $R_z$  indicate a smooth and uniform film surface,  
348 which is generally important for ideal packaging film<sup>44</sup>. These combined changes of  
349 SEM and optical profilometry, suggests that TE modifies the microstructure of film,  
350 leading to enhanced surface texture and altered optical properties<sup>6, 45</sup>.

351 < Insert Figure 3>



352 **3.2.2. Optical and barrier attribute analysis STKB and STKTE 0.5% film** View Article Online  
DOI: 10.1039/D5FB00838G

353

354 Colour, opacity and light transmittance are crucial parameters for packaging film  
355 applications, as these impact on the product freshness and consumers perception. A  
356 higher opacity value indicates greater absorption of visible light by the film at a specific  
357 thickness, thereby reducing light transmission through the film. The addition of TE  
358 changes color of the film and also impacted the % transmittance and opacity of the  
359 film (**Figure 4**). The colorimetric analysis revealed that the STKTE 0.5% sample  
360 exhibits a noticeable yellow coloration, with high  $b^*$  value (42.90) and positive  $a^*$  value  
361 (17.24), along with a lower lightness value ( $L^* = 51.92$ ) compared to the almost  
362 colorless STKB sample ( $L^* = 87.89$ ). The large color difference ( $\Delta E = 51.16$ ) between  
363 the two samples confirms the visible color change upon TE addition<sup>6</sup>.

364

**< Insert Figure 4>**

365 The ultraviolet (UV) radiation significantly contributes to the deterioration of food  
366 quality; hence, packaging films should offer sufficient transparency while effectively  
367 blocking UV light to ensure product preservation. The UV-blocking capability of the  
368 films was assessed using a UV spectrophotometer <sup>13</sup>. The results revealed that  
369 STKTE 0.5% film completely absorbed the UV region light (UVA, UVB and UVC light)  
370 and demonstrated negligible transmittance across the film. This remarkable UV  
371 blocking ability of the STKTE 0.5% was due to the polyphenolic constituents present  
372 in the TE which effectively absorb ultraviolet radiation <sup>40, 46</sup>. The incorporation of 0.5%  
373 TE into STKB not only improves UV protection but also imparts a distinct yellow tint  
374 and reduces the lightness of the film. Similarly, the STKTE 0.5% film showed high  
375 opacity value  $0.039 \pm 0.00007$  as compare to STKB film ( $0.028 \pm 0.0002$ ) (**Figure 5a**).  
376 This confirms that in STKTE 0.5% film, addition of tea extract (TE) improved the light  
377 absorbing property of the films.

378 Further, the ability of packaging films to restrict the transmission of water and gases  
379 is a critical determinant of their effectiveness in food preservation. Among these, water  
380 barrier properties are particularly important, as they help maintain the moisture  
381 balance, texture, and overall stability of food products during storage <sup>28, 47</sup>. These  
382 characteristics are commonly evaluated through measurements of moisture content,  
383 WVP and oxygen permeability. The WVP of a film is largely governed by its thickness,



384 degree of crosslinking, and polymer chain mobility. Additionally, oxygen exposure can  
385 accelerate undesirable processes such as lipid oxidation, discoloration, and microbial  
386 growth, ultimately leading to food spoilage <sup>48</sup>. Collectively, these factors are essential  
387 for preserving the freshness, sensory quality, and nutritional value of foods while  
388 extending their shelf life. Therefore, the developed films were assessed for these  
389 parameters to comprehensively evaluate their barrier performance.

390 The results revealed that the moisture content % of the STKTE 0.5% film ( $17.16 \pm 0.44$   
391 %) significantly reduced compared to STKB film ( $22.28 \pm 1.94$  %) (**Figure 5b**). The  
392 decrease in the moisture content % of the tea extract loaded (STKTE 0.5%) film, due  
393 to the inclusion of the hydrophobic constituents of TE, which lowers the water  
394 adsorption capability of the film. Similar results were reported by wen et al., in their  
395 study on pH-sensitive Poly (vinyl alcohol) films incorporated with green tea extract <sup>40</sup>.  
396 Similarly, notable decrease in WTR and OTR of the STKTE 0.5% was observed  
397 (**Figure 5c and d**). Specifically, the STKTE 0.5% film exhibited significantly lower WVP  
398 ( $1.68 \pm 0.07 \times 10^{-7}$ .g.mm/sec.m<sup>2</sup>.Pa) than STKB film ( $2.17 \pm 0.12 \times 10^{-7}$ .g.mm/sec.m<sup>2</sup>.Pa).  
399 The WVP of the STKTE 0.5% film was decreased due to addition of TE containing  
400 bulky aromatic skeleton and can obstruct the inner network of the tea extract loaded  
401 film (STKTE 0.5%), corresponds to lower vapor affinity of the films <sup>40, 42</sup>. The oxygen  
402 permeability of the films followed the similar trend as the WTR. The STKTE 0.5% film  
403 exhibited significant decrease ( $5.97 \pm 0.63 \times 10^{-6}$ .g.mm/m<sup>2</sup>.s) in the oxygen permeability  
404 as compared to STKB film ( $13.07 \pm 1.18 \times 10^{-6}$ .g.mm/m<sup>2</sup>.s). The TE present in the  
405 STKTE 0.5% film, acted as a barrier that successfully inhibited the diffusion of the  
406 oxygen molecules, which corresponds to lower oxygen permeability. Also, the  
407 crosslinking of the film materials, reduced the free space present in the film, resulted  
408 in low OP values<sup>14</sup>. These findings indicated that the addition of 0.5% TE not only  
409 increases film opacity but also enhances its moisture resistance and gas barrier  
410 performance, making the modified film potentially more suitable for packaging  
411 applications.

412 < Insert Figure 5>

413 **3.2.3. Molecular, solid state and thermal analysis of STKB and STKTE 0.5% films**

414 The FTIR spectra of the film and film components were analysed to understand the  
415 intermolecular interaction between the components of films (**Figure 6a**). The FTIR  
416 spectra of starch showed band at  $3399\text{ cm}^{-1}$  and  $2929\text{ cm}^{-1}$  corresponding to the  
417 symmetric and asymmetric stretching vibrations of O-H and C-H groups. The  
418 absorption peak at  $991\text{ cm}^{-1}$  was attributed to the hydrogen bond formed by oxygen  
419 atom on the starch glycosidic bond <sup>5, 23, 49</sup>. The FTIR spectrum of the PVA-PEG  
420 copolymer (KIR) showed a broad and intense absorption band between 3600 and  
421  $3000\text{ cm}^{-1}$ , related to O-H stretching vibrations, indicative of strong hydrogen bonding  
422 interactions. Two distinct peaks at  $2897.18\text{ cm}^{-1}$  and  $1433.04\text{ cm}^{-1}$  were attributed to  
423 asymmetric  $\text{CH}_2$  stretching and CH-O-H bending vibrations, contributed to its  
424 polymeric backbone structure. Additionally, two characteristic peaks at  $1241.50\text{ cm}^{-1}$   
425 and  $1084.05\text{ cm}^{-1}$  corresponds to C-O-C stretching of the alkyl ether group and C-O  
426 stretching vibrations, respectively <sup>17, 50</sup>. The FTIR spectra of TE demonstrated the  
427 absorption at  $1350\text{ cm}^{-1}$  and  $1446\text{ cm}^{-1}$ , which attributed to C-H stretching and peak  
428 at  $1647\text{ cm}^{-1}$  contributed to c=C stretching <sup>40</sup>. The FTIR spectra of STKB and STKTE  
429 0.5% film exhibited the broadening and shifting of peaks of film components in the  
430 region between  $3700 - 3000\text{ cm}^{-1}$  and  $1500 - 1800\text{ cm}^{-1}$  demonstrating possible  
431 hydrogen bonding linkage between the film polymers.

432 The crystal structures of the ST, PVA-PEG copolymer (KIR), STKB, STKTE 0.5% were  
433 determined using XRD analysis (**Figure 6b**). The XRD pattern of ST exhibited high  
434 intensity peak at 17 and low intensity peaks at 15, 22.6 and 24.2, demonstrating its  
435 partial crystalline nature <sup>5, 23</sup>. On the other hand, the diffractogram of KIR attributed  
436 only one defused pattern at 19.3 and 22 ( $2\theta$ ), typical of semi-crystalline polymeric  
437 structures <sup>51</sup>. Similarly, the XRD spectra of TE demonstrated its partial amorphous  
438 nature due to the presence of numerous components including fibres, tea polyphenols  
439 and catechins. Further, the XRD diffractogram of film samples (STKB and STKTE  
440 0.5%) demonstrated diffused and halo spectra, revealing amorphization of the film  
441 components. This transition toward an amorphous structure reflects strong interfacial  
442 interactions between the components, which may enhance material uniformity and  
443 performance.

444 The thermal stability of the developed films was analyzed by thermogravimetric  
445 analysis. TGA thermogram of all samples demonstrated multi-step degradation,



446 typically involving initial moisture loss followed by the decomposition of the organic  
447 matrix (**Figure 6c**). Specifically, degradation of ST initiated at 246.1 °C to 378.5 °C  
448 and 378.5 °C -548.7 °C corresponding to 52.1 % and 27.21 % weight loss with residual  
449 weight of 7.19 %, respectively <sup>25, 52</sup>. The TGA profile of PVA-PEG copolymer (KIR)  
450 exhibited a distinct two-step degradation pattern <sup>53</sup>. The initial stage showed a minor  
451 weight loss of approximately 1.3% below 150 °C, corresponding to the evaporation of  
452 physically adsorbed and bound water molecules. The primary decomposition phase  
453 occurred between 163 °C and 432.6°C, resulting in a weight loss of about 81.33%,  
454 which can be attributed to the degradation of organic constituents and partial cleavage  
455 of the polymer backbone. Subsequent degradation events between 432.6°-483.2 °C  
456 and 483.2 °C-550 °C contributed additional weight losses of 6.17% and 10.6%,  
457 respectively. The thermogram of TE displayed a broad degradation band beginning at  
458 around 150 °C, with a peak near 200 °C till 392 °C corresponding to 95 % weight loss.  
459 This transition is attributed to the thermal decomposition of glycosylated catechins,  
460 where the attached sugars undergo caramelization upon heating. Additionally, the  
461 partial degradation of catechins, leading to the formation of gallic acid and subsequent  
462 polymerization of phenolic compounds, contributes to this thermal event. The  
463 degradation extended over a wide temperature range, with a final stage observed  
464 beyond 340 °C, corresponding to the thermal decomposition of cellulose components  
465 present in the TE<sup>40</sup>.

466 The thermal stability of the film samples improved upon the incorporation of TE in film  
467 components, as observed in the STKTE 0.5% curves, which exhibit delayed onset of  
468 degradation from 200°C (in TE) to 229 °C. Moreover, the TGA curve of STKTE 0.5%  
469 curves demonstrated gradual increase in weight loss in despite of sharp increase in  
470 degradation as observed in TE curve. This enhancement can be attributed to the  
471 reinforcing effect and thermal barrier properties imparted by the additives.

472 Overall, the combined FTIR, XRD, and TGA results confirm the successful integration  
473 of PVA-PEG copolymer (KIR) and TE into the ST matrix, leading to chemical  
474 interactions, reduced crystallinity, and improved thermal stability. These modifications  
475 suggest that the composite film enhanced the structural homogeneity and thermal  
476 resistance compared to the unmodified samples.

477



478

View Article Online  
DOI: 10.1039/D5FB00838G479 **3.3. Antioxidant activity and biocompatibility of STKB and STKTE 0.5% films**

480 The antioxidant ability (free radical scavenging activity) is crucial for food packaging  
481 films, as free radicals generated in food can cause oxidation and spoilage of food. The  
482 DPPH radical scavenging activity is important to estimate antioxidant property of film  
483 samples. The results demonstrated that DPPH scavenging activity of STKTE 0.5%  
484 film exhibited concentration dependent increase as compared to STKB film, with 84%  
485 scavenging at the highest concentration (1000  $\mu$ g/mL) (**Figure 7a**). However, STKB  
486 film showed only 7 % scavenging at highest concentration (1000  $\mu$ g/mL). The addition  
487 of TE improved the antioxidant potential of the film (STKTE 0.5%), due to the presence  
488 of phenolic compounds present in TE. The TE components are known to disrupt chain  
489 oxidation reaction, releasing hydrogen atom and acts as a receptor for free radicals <sup>13,</sup>  
490 <sup>27, 54</sup>. This suggested that the addition of TE significantly influenced the antioxidant  
491 activity of the films.

492 To determine the cytocompatibility of the developed films (STKB and STKTE 0.5%),  
493 *in vitro* biocompatibility was performed using L929 mouse fibroblast cell line. The film  
494 samples were incubated with fibroblast cells followed by MTT assay to determine cell  
495 viability. In case of both films (STKB and STKTE 0.5%) the cell viability observed was  
496 more than 90%, suggesting that films are biocompatible and non- toxic to cells (**Figure**  
497 **7b**). Despite the incorporation of tea extract (TE), STKTE 0.5% film sample maintained  
498 high cell compatibility, demonstrating that neither its concentration nor its incorporation  
499 method induced any adverse cellular response <sup>21, 55</sup>. The excellent biocompatibility of  
500 these films supports their potential role for interaction with biological tissues extending  
501 their application beyond the food packaging.

502

**<Insert Figure 7>**503 **3.4. Tea extract migration analysis**

504 In general, the release/migration of active component from the film is critical for  
505 providing effective functional attributes to film. This migration also depends upon the  
506 type of food preserved in the packaging material and its rate depends upon  
507 compatibility between film polymer, food simulant and active component <sup>37</sup>. Therefore,



508 the migration of TE from STKTE 0.5% films was analyzed in three different food  
509 simulants (3% acetic acid, 95% ethanol and water) (Supplementary table S1). The  
510 results of migration study revealed that film in 3% acetic acid ( $79.7 \pm 2.0\%$ ) and water  
511 simulant ( $77.3 \pm 2.7\%$ ) showed maximum release/migration of TE from film to solution.  
512 However, the film incubated in 95% ethanol demonstrated  $51.5 \pm 4.4\%$  migration of  
513 TE, possibly because of the limited solubility of starch in ethanol. Further, the DPPH  
514 assay of the simulant solution also confirmed the effective migration and retention of  
515 antioxidant activity of films (Supplementary figure S1). Specifically, antioxidant assay  
516 results revealed that film in 3% acetic acid ( $80.1 \pm 0.2\%$ ) and water ( $72.7 \pm 0.2\%$ )  
517 demonstrated highest and equivalent DPPH scavenging activity to that of STKTE  
518 0.25% film without simulant treatment in comparison to film in 95% ethanol simulant  
519 ( $60.1 \pm 0.2\%$ ). The higher antioxidant activity in acetic acid and water, may be  
520 because of the higher solubility of film in these simulants in comparison to ethanol.  
521 The starch alone is usually less soluble in water, but the incorporation of the PVA-PEG  
522 copolymer increased its solubility by forming hydroxyl groups and allows the  
523 antioxidant compounds to release more effectively from film samples<sup>56</sup>. The similar  
524 results were obtained in a study conducted on mixing the potato starch with PVA,  
525 which results in formation of hydrophilic films and increase the solubility of films in  
526 water, mainly because of increase in number of -OH groups<sup>57</sup>.

### 527 3.5. Antibacterial efficiency of STKB and STKTE 0.5% films

528 The antibacterial properties of developed films can inhibit the growth of potential  
529 foodborne pathogen, thereby limit the foodborne illnesses and prolong the food shelf-  
530 life. The antibacterial efficiency of developed films was tested against two bacterial  
531 strains: *S. aureus* (Gram-positive) and *E. coli* (Gram-negative) bacteria and  
532 determined by colony Forming Unit (CFU/mL) method (**Figure 8**). The control and  
533 STKB film exhibited intense bacterial growth in comparison to STKTE 0.5% against  
534 both the bacterial strains (*S. aureus* and *E. coli*). Specifically, the STKTE 0.5% film  
535 showed,  $7.9 \times 10^6$  CFU/mL against *S. aureus* and  $3.3 \times 10^6$  CFU/mL against *E. coli*,  
536 which indicates that STKTE 0.5% film exhibited significant antibacterial effect against  
537 *E. coli* as compared to *S. aureus* (**Figure 8**). The results demonstrated that developed  
538 STKTE 0.5% film showed promising inhibition on growth of both the bacterial strains  
539 in comparison to STKB film. The antibacterial property of the STKTE 0.5% film can be



540 attributed to incorporation of the TE, which contain polyphenols, and have the potential  
541 to inhibit the growth of wide variety of bacteria especially gram-positive and gram-  
542 negative species <sup>13</sup>. The observed results are supported by the findings of Lie et al.,  
543 reported the significant inhibition of *E. coli* than *S. aureus* at equivalent concentration  
544 of TE <sup>24</sup>.

View Article Online  
DOI:10.1039/D9FO00838G

545 **<Insert Figure 8>**

546 **3.6. Fresh cut apple preservation**

547 The ability of the STKB and STKTE 0.5% films to preserve fresh cut apple was  
548 examined by monitoring several quality parameters viz., visual appearance, color  
549 parameters, % weight loss, pH and BI<sup>32</sup>. In terms of visual appearance, the fruits  
550 packed in STKTE 0.5% film effectively maintained their appearance till the 5<sup>th</sup> day of  
551 experiment followed by STKB, PE and control groups (**Figure 9a**). Moreover, the color  
552 parameters ( $L^*a^*b^*$  values) of the apple cubes were also in corroboration with the visual  
553 appearance, confirming the color changes during storage (**Figure 9b**). Further, the  
554 browning index of apple was also evaluated and results demonstrated browning index  
555 of apple cubes was highest in control as the fruit cubes were not protected. However,  
556 in case of covered fruit cubes the browning index decreased from PE > STKB >STKTE  
557 0.5% (**Figure 9c**). The possible cause of fruit browning could be the polyphenols  
558 oxidation to produce quinones which reacts to generate brown/ black pigments <sup>33, 58</sup>.

559 The weight loss assessment of stored apple cubes was also estimated for a period of  
560 5 days and it was observed that the weight loss was maximum ( $57.1 \pm 10.4$ ) in the  
561 control group (uncovered apple cubes). In contrast the covered apple cubes exhibit  
562 minimum weight loss starting from PE ( $52.0 \pm 10.7$ ) followed by STKB ( $30.2 \pm 6.6$ ) and  
563 then STKTE 0.5% ( $28.6 \pm 6.4$ ) (**Figure 9d**). The weight loss observed in all the groups,  
564 is likely to be associated with the rapid increase in respiration just after the cutting of fruit.  
565 Moreover, since moisture loss is directly associated with film permeability, the weight  
566 loss results can be interpreted on basis of WVP values <sup>58, 59</sup>. The film with lower WVP  
567 (STKTE 0.5%) exhibited least weight loss, whereas STKB film with higher WVP  
568 showed greater weight loss than STKTE 0.5%.

569 The pH serves as a key indicator of fruit freshness and spoilage. The decline in apple  
570 pH during storage is primarily attributed to the accumulation of acidic metabolites,



571 enzymatic breakdown of cell wall components, and potential microbial fermentation.  
572 Together, these processes elevate the fruit's overall acidity, signalling progressive  
573 deterioration in quality<sup>32</sup>. Therefore, the pH of apple was estimated at the end of the  
574 experiment, revealing that the pH in control group found to be the lowest ( $2.47 \pm 0.03$ )  
575 as compare to other groups. The STKTE 0.5% group found best to maintain the pH  
576 ( $2.63 \pm 0.02$ ) of the fruits (**Figure 9d**) in comparison to blank ( $2.53 \pm 0.05$ ) and  
577 commercial packaging film ( $2.48 \pm 0.04$ ).

578 **<Insert Figure 9>**

579 **3.7. Soil burial test assessment**

580 The physical disintegration assessment of the STKB and STKTE 0.5% films was  
581 carried out using soil burial method for a period of 10 days<sup>34</sup>. The STKTE 0.5% film  
582 showed significant reduction in film area with residual area of  $0.6 \pm 0.6\%$  as compare  
583 to STKB film ( $3.4 \pm 2.0\%$ ), confirming its high vulnerability towards microbial  
584 degradation and breakdown in environmental conditions (**Figure 10**). Overall, both the  
585 films STKB, STKTE 0.5% showed the potential to serve as sustainable alternatives for  
586 conventional food packaging materials.

587 **<Insert Figure 10>**

588 **4. Conclusion**

589 In nutshell, the study presents the successful development of biodegradable and  
590 functional films based on starch and PVA-PEG (Kollicoat IR) copolymer incorporated  
591 with green tea extract (TE) as a natural bioactive additive. The incorporation of 0.5%  
592 w/v TE markedly enhanced the mechanical strength, water contact angle and barrier  
593 properties of the films, demonstrating superior performance compared to the blank  
594 STKB film. The structural and thermal analyses (SEM, 3D profilometry, FTIR, XRD,  
595 and TGA) confirmed improved film uniformity, strong intermolecular interactions, and  
596 enhanced thermal stability upon TE addition. The developed films exhibited enhanced  
597 antioxidant and antibacterial activities, effectively inhibiting *E. coli* and *S. aureus*, while  
598 maintaining cytocompatibility in L929 fibroblast cells. The application of the films for  
599 packaging fresh-cut apples significantly reduced browning, weight loss, and pH  
600 decline, indicating extended shelf life and improved preservation quality. Moreover,



601 the films displayed rapid physical disintegration within 10 days under soil burial  
602 conditions, confirming their environmental sustainability. Overall, the developed  
603 ST/PVA-PEG/TE films present a promising green alternative to conventional plastic  
604 packaging, combining biodegradability, bioactivity, and functional performance  
605 suitable for food preservation and sustainable packaging applications.

[View Article Online](#)  
DOI: 10.1039/D9FB00838G

## 606 **Supplementary Information**

607 Supplementary information includes table of percent migration of tea extract from  
608 STKTE 0.5% film and figure of DPPH assay of film samples after migration study  
609 conducted for 10 days in different food simulants (3% Acetic acid, water and 95%  
610 ethanol).

## 611 **Data Availability Statement**

612 Data supporting the findings of this study are available within the manuscript.

## 613 **CRediT authorship contribution statement**

614 **Neha Rana:** Writing - original draft, Methodology, Investigation, Data curation, Formal  
615 analysis. **Ruchika:** Methodology, Investigation, Writing - original draft, Formal  
616 analysis. **Ankit Saneja:** Writing - review & editing, Supervision, Project administration,  
617 Funding acquisition, Conceptualization.

## 618 **Declaration of Competing Interest**

619 The authors declare that they have no known competing financial interests or personal  
620 relationships that could have appeared to influence the work reported in this paper.

## 621 **Acknowledgement**

622 The authors acknowledge Director CSIR-Institute of Himalayan Bioresource  
623 Technology for his support. The authors are thankful to the Council of Scientific and  
624 Industrial Research (CSIR), New Delhi, for financial assistance under the MLP-204  
625 project. Figure 1 and graphical abstract of the manuscript was created using  
626 BioRender.com. During the preparation of this article, the author(s) used "Grammarly"  
627 to improve the language of the manuscript with appropriate caution. The author(s)  
628 reviewed and edited the content after using the tool and take full responsibility for the  
629 final version of the published article.



630

631

632 **5. References**

- 633 1. H. Baniasadi, R. Abidnejad, M. Fazeli, J. Niskanen and E. Lizundia, *Materials*  
634 *Science Engineering: R: Reports*, 2026, **167**, 101128.
- 635 2. M. Anwar, M. E. Konnova and S. Dastgir, *RSC Sustainability*, 2025.
- 636 3. W. Zhang, J. Yang, M. Ghasemlou, Z. Riahi, A. Khan, G. Goksen, Y. Zhang  
637 and J.-W. Rhim, *Materials Science Engineering: R: Reports*, 2025, **166**,  
638 101068.
- 639 4. P. Kalita, N. S. Bora, B. Gogoi, A. Goswami, L. Pachuau, P. J. Das, D. Baishya  
640 and S. Roy, *Food Chemistry*, 2025, 143793.
- 641 5. Y. Ma, H. Zhao, Q. Ma, D. Cheng, Y. Zhang, W. Wang, J. Wang and J. Sun,  
642 *Food Packaging Shelf Life*, 2022, **31**, 100793.
- 643 6. A. Khan, P. Ezati and J.-W. Rhim, *ACS Applied bio materials*, 2023, **6**, 1294-  
644 1305.
- 645 7. H. Deng, J. Su, W. Zhang, A. Khan, M. A. Sani, G. Goksen, P. Kashyap, P.  
646 Ezati and J.-W. Rhim, *International Journal of Biological Macromolecules*,  
647 2024, **273**, 132926.
- 648 8. X. Zhao, Y. Wang, X. Chen, X. Yu, W. Li, S. Zhang, X. Meng, Z.-M. Zhao, T.  
649 Dong and A. Anderson, *Matter*, 2023, **6**, 97-127.
- 650 9. A. A. Hunashyal, S. P. Masti, M. P. Eelager, O. J. D'souza, L. K. Kurabetta, M.  
651 N. Gunaki, S. Madihalli, J. P. Pinto, M. B. Megalamani and R. B. Chougale,  
652 *Next Nanotechnology*, 2025, **8**, 100292.
- 653 10. S. Phattarateera, R. Wungpunya, S. Thongkhlaeo, L. Tatong, C. Thongpin and  
654 P. Threepopnatkul, *Journal of Polymer Research*, 2025, **32**, 390.
- 655 11. M. Sharma, P. Beniwal and A. P. Toor, *Materials Chemistry Physics*, 2022, **291**,  
656 126652.
- 657 12. C. Xu, S. Zhou, H. Song, H. Hu, Y. Yang, X. Zhang, S. Ma, X. Feng, Y. Pan  
658 and S. Gong, *Nano Today*, 2023, **52**, 101990.
- 659 13. P. Shan, K. Wang, F. Yu, L. Yi, L. Sun and H. Li, *Colloids Surfaces A: Physicochemical Engineering Aspects*, 2023, **662**, 131013.
- 660 14. J. R. Ansari, K. Park and J. Seo, *Food Packaging Shelf Life*, 2025, **48**, 101460.



Open Access Article. Published on 08 January 2026. Downloaded on 1/12/2026 5:31:15 AM.  
This article is licensed under a Creative Commons Attribution-NonCommercial 3.0 Unported Licence.

Article Online  
DOI: 10.1659/DBF-B00838G

662 15. J. Wu, S. Chen, S. Ge, J. Miao, J. Li and Q. Zhang, *Food hydrocolloids*, 2013,  
663 **32**, 42-51.

664 16. M. A. Andrade, C. H. Barbosa, M. A. Cerqueira, A. G. Azevedo, C. Barros, A.  
665 V. Machado, A. Coelho, R. Furtado, C. B. Correia, M. J. F. P. Saraiva and S.  
666 Life, 2023, **36**, 101041.

667 17. A. J. Mali, S. Patil and B. Chellampillai, *Journal of Polymer Research*, 2022, **29**,  
668 130.

669 18. A. L. Vicario, M. G. Garcia, N. A. Ochoa and E. Quiroga, *Food Hydrocolloids*,  
670 2024, **153**, 110009.

671 19. A. Aragón-Gutiérrez, L. Higueras-Contreras, G. López-Carballo, A. Gómez-  
672 García, M. Gallur, D. López, R. Gavara and P. Hernández-Muñoz, *Food  
673 Packaging Shelf Life*, 2024, **46**, 101355.

674 20. N. Khan and A. Saneja, *Journal of Molecular Structure*, 2025, 142652.

675 21. S. Ruchika, Sanjeev Kumar, R. Kumar, S. K. Yadav and A. Saneja,  
676 *International Journal of Biological Macromolecules*, 2025, **293**, 139241.

677 22. N. Deng, Z. Hu, H. Li, C. Li, Z. Xiao, B. Zhang, M. Liu, F. Fang, J. Wang and Y.  
678 Cai, *International Journal of Biological Macromolecules*, 2024, **260**, 129340.

679 23. Y. Wang, H. Zhang, Y. Zeng, M. A. Hossen, J. Dai, S. Li, Y. Liu and W. Qin,  
680 *Food Packaging Shelf Life*, 2022, **33**, 100837.

681 24. Y. Lei, H. Wu, C. Jiao, Y. Jiang, R. Liu, D. Xiao, J. Lu, Z. Zhang, G. Shen and  
682 S. Li, *Food Hydrocolloids*, 2019, **94**, 128-135.

683 25. K. Yogananda, E. Ramasamy and D. Rangappa, *Ionics*, 2019, **25**, 6035-6042.

684 26. S. R. Kanatt, M. Rao, S. Chawla and A. Sharma, *Food hydrocolloids*, 2012, **29**,  
685 290-297.

686 27. M. Abdin, A. A. Metwally, M. Younis, M. Khalil and S. G. Arafa, *Food Chemistry*,  
687 2025, 147089.

688 28. J. Chen, X. Zhang, H. Lin, G. Chen, W. Zhang and D.-P. Yang, *Chemical  
689 Engineering Journal*, 2025, **511**, 162184.

690 29. C. L. de Dicastillo, M. del Mar Castro-López, J. M. López-Vilariño and M. V. J.  
691 F. r. i. González-Rodríguez, *Food research international*, 2013, **53**, 522-528.

692 30. F. S. Mortazavi Moghadam, S. Rasouli and F. A. Mortazavi Moghadam, *ACS  
693 Food Science Technology*, 2025, **5**, 1024-1041.

694 31. R. Podgórski, M. Wojasiński and T. Ciach, *Scientific reports*, 2022, **12**, 9047.

Open Access Article. Published on 08 January 2026. Downloaded on 1/12/2026 5:31:15 AM.  
This article is licensed under a Creative Commons Attribution-NonCommercial 3.0 Unported Licence.

695 32. T. Almeida, A. Karamysheva, B. F. Valente, J. M. Silva, M. Braz, A. Almeida,  
696 A. J. Silvestre, C. Vilela and C. S. Freire, *Food Hydrocolloids*, 2023, **144**,  
697 108934.

698 33. L. Jiang, F. Wang, X. Xie, C. Xie, A. Li, N. Xia, X. Gong and H. Zhang,  
699 *International Journal of Biological Macromolecules*, 2022, **209**, 1307-1318.

700 34. M. Liu, H. Chen, F. Pan, X. Wu, Y. Zhang, X. Fang, X. Li, W. Tian and W. Peng,  
701 *Carbohydrate Polymers*, 2024, **343**, 122445.

702 35. T. C. Vianna, C. O. Marinho, L. M. Júnior, S. A. Ibrahim and R. P. Vieira,  
703 *International Journal of Biological Macromolecules*, 2021, **182**, 1803-1819.

704 36. R. K. Sidhu, C. Riar and S. Singh, *Sustainable Food Technology*, 2026.

705 37. T. Y. Feng, M. N. Hidayah, F. H. Lyn and Z. N. Hanani, *Sustainable Food  
Technology*, 2025, **3**, 1986-1995.

707 38. R. K. Gupta, P. Guha, P. P. J. P. P. Srivastav and Polymers, 2024, **21**, 2400047.

708 39. Z. Wang, C. Xu, L. Qi and C. Chen, *Trends in Chemistry*, 2024, **6**, 314-331.

709 40. H. Wen, Y.-I. Hsu, T.-A. Asoh and H. Uyama, *Polymer Degradation Stability*,  
710 2020, **178**, 109215.

711 41. Z. Wu, C. Tong, J. Zhang, J. Sun, H. Jiang, M. Duan, C. Wen, C. Wu and J.  
712 Pang, *International Journal of Biological Macromolecules*, 2021, **192**, 323-330.

713 42. H. Wu, Y. Lei, R. Zhu, M. Zhao, J. Lu, D. Xiao, C. Jiao, Z. Zhang, G. Shen and  
714 S. Li, *Food Hydrocolloids*, 2019, **90**, 41-49.

715 43. A. Sadeghi, S. M. A. Razavi and D. Shahrampour, *International Journal of  
Biological Macromolecules*, 2022, **205**, 341-356.

717 44. T. S. Awad, D. Asker and B. D. Hatton, *ACS applied materials interfaces*, 2018,  
718 **10**, 22902-22912.

719 45. A. H. Hashem, M. E. El-Naggar, A. M. Abdelaziz, S. Abdelbary, Y. R. Hassan  
720 and M. S. Hasanin, *International Journal of Biological Macromolecules*, 2023,  
721 **249**, 126011.

722 46. W. Zhang, H. Jiang, J.-W. Rhim, J. Cao and W. Jiang, *Critical reviews in food  
science nutrition*, 2022, **63**, 288-301.

724 47. F. N. Eze, R. C. Eze, S. Singh and K. E. Okpara, *International Journal of  
Biological Macromolecules*, 2024, **278**, 134914.

726 48. Q. Hua, Z. Huang, J. Gou, H. Zhang, I. Therrien, J. Wu, Y. Liang and S.  
727 Renneckar, *Chemical Engineering Journal*, 2024, **499**, 156139.

728 49. R. Abedi-Firoozjah, N. Chabook, O. Rostami, M. Heydari, A. Kolahdouz-Nasiri, *View Article Online*  
729 F. Javanmardi, K. Abdolmaleki and A. M. Khaneghah, *Polymer testing*, 2023,  
730 **118**, 107903.  
731 50. P. Desai and B. Chatterjee, *ACS omega*, 2023, **8**, 45337-45347.  
732 51. S. Janssens, H. N. de Armas, J. P. Remon and G. Van den Mooter, *European*  
733 *journal of pharmaceutical sciences*, 2007, **30**, 288-294.  
734 52. B. Schmidt, K. Kowalczyk and B. Zielinska, *Materials*, 2021, **14**, 1498.  
735 53. D. Kramarczyk, J. Knapik-Kowalczuk, M. Kurek, W. Jamróz, R. Jachowicz and  
736 M. Paluch, *Pharmaceutics*, 2023, **15**, 799.  
737 54. V. Hemmati, F. Garavand, N. Khorshidian, I. Cacciotti, M. Goudarzi, M. Chaichi  
738 and B. K. Tiwari, *Food Bioscience*, 2021, **44**, 101348.  
739 55. E. P. Bavi, E. Shakerinasab, H. Hamidinezhad and E. Nazifi, *International*  
740 *Journal of Biological Macromolecules*, 2023, **224**, 1183-1195.  
741 56. S. Patil, A. K. Bharimalla, A. Mahapatra, J. Dhakane-Lad, A. Arputharaj, M.  
742 Kumar, A. Raja and N. Kamblu, *Food Bioscience*, 2021, **44**, 101352.  
743 57. C. A. Gómez-Aldapa, G. Velazquez, M. C. Gutierrez, E. Rangel-Vargas, J.  
744 Castro-Rosas and R. Y. Aguirre-Loredo, *Materials Chemistry Physics*, 2020,  
745 **239**, 122027.  
746 58. M. El Mouzahim, E. Eddarai, S. Eladaoui, A. Guenbour, A. Bellaouchou, A.  
747 Zarrouk and R. Boussen, *International Journal of Biological Macromolecules*,  
748 2023, **233**, 123430.  
749 59. Y. Guan, Y. Ji, X. Yang, L. Pang, J. Cheng, X. Lu, J. Zheng, L. Yin and W. Hu,  
750 *LWT*, 2023, **175**, 114478.  
751  
752  
753  
754  
755  
756



757

758

759 **Figure legends**

Figure	Legend
<b>Figure 1</b>	(a) Schematic illustration of development of starch/PVA-PEG copolymer packaging film reinforced with green tea extract and its assessment for mechanical, barrier and solid-state characterization. (b) The developed film was further analysed for functional properties including antioxidant and antibacterial, postharvest apple preservation, biocompatibility and biodegradability.
<b>Figure 2</b>	Mechanical and surface properties of STKB and STKTE films with varying concentrations of green tea extract (TE). (a) Representative stress-strain curves demonstrate the mechanical behavior of the samples under tensile loading. (b) Tensile strength, (c) elongation at break, and (d) water contact angle measured for STKB and STKTE films containing 0.25%, 0.5%, and 1% w/v of TE. Data are presented as mean $\pm$ standard deviation ( $n = 3$ ). Statistically significant differences are indicated by different letters above the bars: “a” denotes a significant difference from STKB, “b” from STKTE 0.25%, and “c” from STKTE 0.5%. In d) graph representative images of water droplets used for contact angle measurements are shown above each corresponding bar.
<b>Figure 3</b>	Optical appearance, surface morphology, and topography of STKB and STKTE 0.5% films. The STKB film (a) appears highly transparent in the photographic image, allowing clear visibility of printed text under it. The corresponding SEM image, reveals a relatively smooth surface with some dispersed features. Optical profilometry of the STKB film shows a moderately uniform surface with height variations ranging from $-36.6857 \mu\text{m}$ to $5.83474 \mu\text{m}$ . In contrast, the STKTE 0.5% film (b) shows a distinct yellowish tint in the photographic image and reduced transparency. The SEM image at the same magnification



View Article Online  
DOI: 10.1089/DB.0838G

indicates a more heterogeneous surface with more irregular features suggesting increased surface roughness. This is further confirmed by the optical profilometry data, which reveals a less uniform surface topology with height differences ranging from  $-35.9652\text{ }\mu\text{m}$  to  $4.71027\text{ }\mu\text{m}$ .

**Figure 4** Optical and colorimetric properties of STKB and STKTE 0.5% films. (a) UV-visible transmittance spectra, where STKTE 0.5% exhibits significantly reduced transmittance across the UV region (UV-C to UV-A), indicating enhanced UV-shielding compared to STKB. (b) The CIE Lab\* color coordinates, with STKTE 0.5% shifting markedly toward the red-yellow quadrant, while STKB remains near the neutral centre. (c) photographic images of both films and their corresponding colorimetric values. STKTE 0.5% shows a much lower lightness ( $L^*$ ) and higher chromaticity ( $a^*$ ,  $b^*$ ), resulting in a notable color difference ( $\Delta E = 51.16$ ) relative to STKB.

**Figure 5** The comparison of physical and barrier properties between STKB and STKTE 0.5% films. (a) Opacity of the films increased significantly with the addition of 0.5% STKTE, indicating higher light-blocking capability. (b) Moisture content was significantly reduced in the STKTE 0.5% films compared to STKB, suggesting improved water retention characteristics. (c) Water vapor permeability (WVP) decreased in STKTE 0.5% films, indicating enhanced barrier properties against moisture. (d) Oxygen permeability (OP) was also significantly lower in the STKTE 0.5% films, reflecting better resistance to gas transmission. Data are presented as mean  $\pm$  standard deviation ( $n = 3$ ), and bars with “a” indicate statistically significant differences ( $p < 0.05$ ) from STKB film.

**Figure 6** Solid state characterization of ST, KIR, TE, STKB, and STKTE 0.5% samples. (a) Fourier-transform infrared spectroscopy (FTIR) spectra showing characteristic functional groups and chemical interactions among the materials. (b) X-ray diffraction (XRD) patterns highlight the crystallinity and structural changes of the samples. (c)



Thermogravimetric analysis (TGA) curves displaying thermal stability and decomposition profiles as a function of temperature.

**Figure 7** Antioxidant activity and biocompatibility of STKB and STKTE. (a) DPPH scavenging assay shows dose-dependent antioxidant activity for STKTE (0.5%), significantly higher than STKB at all concentrations ( $p < 0.05$ ). (b-i) L929 cell viability graph and (ii) Fluorescence images demonstrate predominantly live cells (green) supporting the biocompatibility of both extracts. The Scale bar in the microscopic images is of 50  $\mu\text{m}$ .

**Figure 8** Antibacterial effects of STKB and STKTE 0.5% against *S. aureus* and *E. coli*. (a) Representative agar plates of *E. coli* demonstrate dose-dependent bacterial inhibition, with reduced colony formation in both strains and Growth curves ( $\text{OD}_{600}$ ) demonstrated both treatments reduce bacterial growth over 12 h compared to control, with STKTE exhibiting stronger inhibition (b) Representative agar plates of *S. aureus* demonstrate dose-dependent bacterial inhibition, with reduced colony formation in both strains, particularly *E. coli*, at higher concentrations of STKTE and Growth curves ( $\text{OD}_{600}$ ) over 12 h compared. (a  $p < 0.05$  vs. control; b  $p < 0.05$  vs. KIRB).

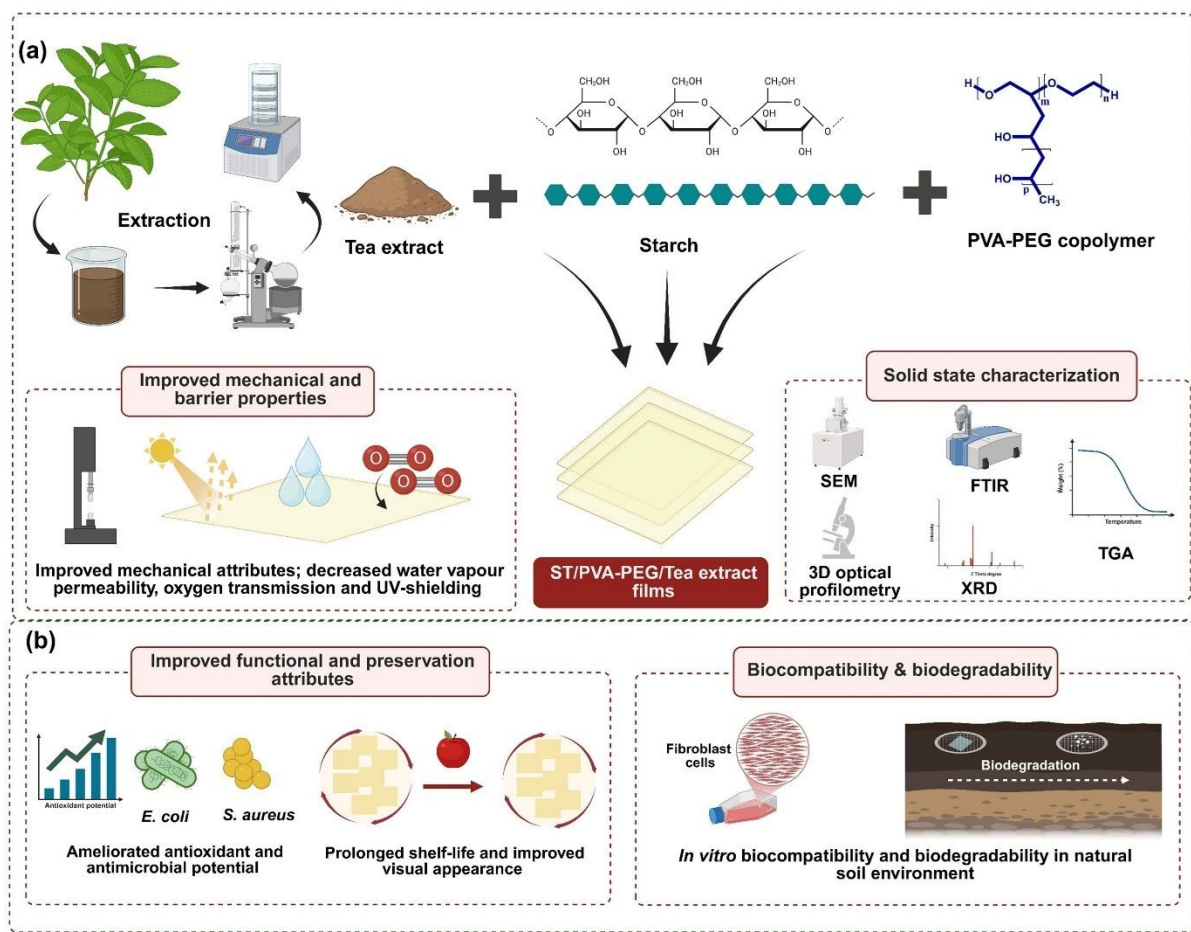
**Figure 9** Effects of different treatments on the quality of fresh-cut apples over 5 days of storage. (a) Visual appearance shows that STKTE 0.5% best preserved color and texture, while the control showed the most browning. (b) Heatmaps of color values ( $L^*$ ,  $a^*$ ,  $b^*$ ) indicate that STKTE 0.5% retained lightness and color better than other treatments. (c) Browning index increased in all samples, but was lowest in STKTE 0.5%. (d) Weight loss was highest in the control and lowest in STKTE 0.5%, indicating improved moisture retention. (e) Graph depicting change in pH of fruit after the storage of 5 days. (a  $p < 0.05$  vs. control; b  $p < 0.05$  vs. KIRB).

**Figure 10** Soil burial test assessment of STKB and STKTE 0.5% films over time. (a) Representative images showing the physical degradation of STKB and STKTE 0.5% films over a 10-day period. (b) Quantitative analysis of % residual area for STKB (green line) and STKTE 0.5% (blue line)



films over time. Data represent mean  $\pm$  standard deviation ( $n = 3$ ). Article Online DOI: 10.1039/D5FB00838G  
STKTE 0.5% films exhibited slightly faster degradation compared to STKB.

760

761  
762  
**Figure 1**

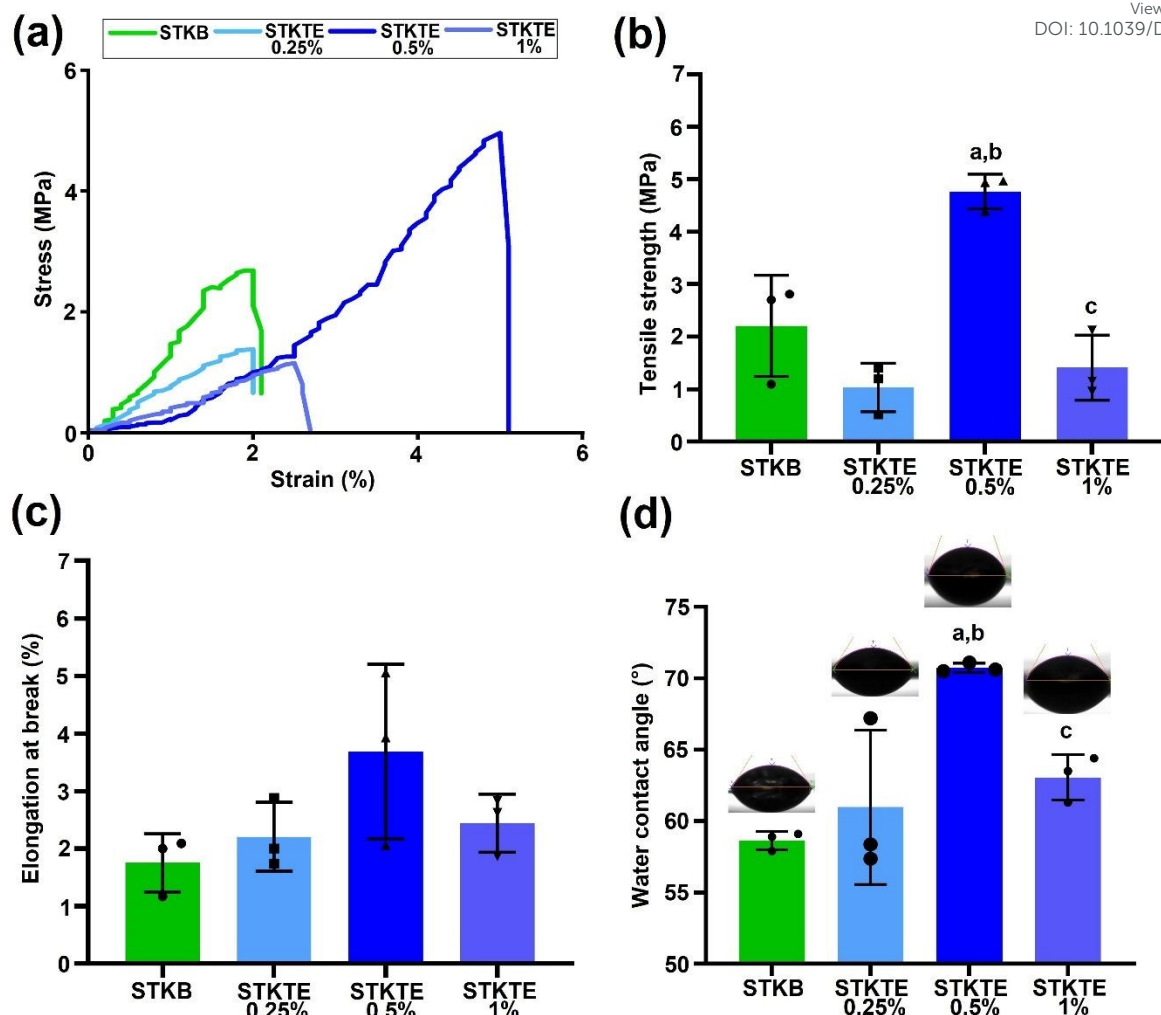


Figure 2



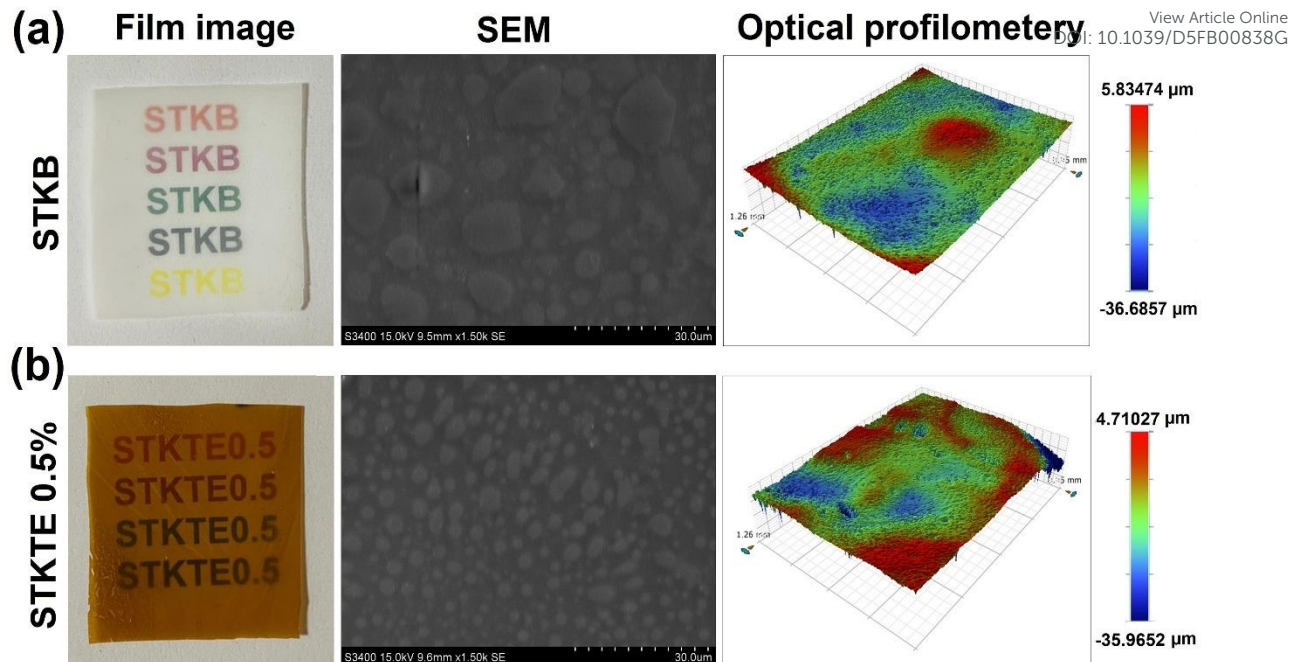


Figure 3

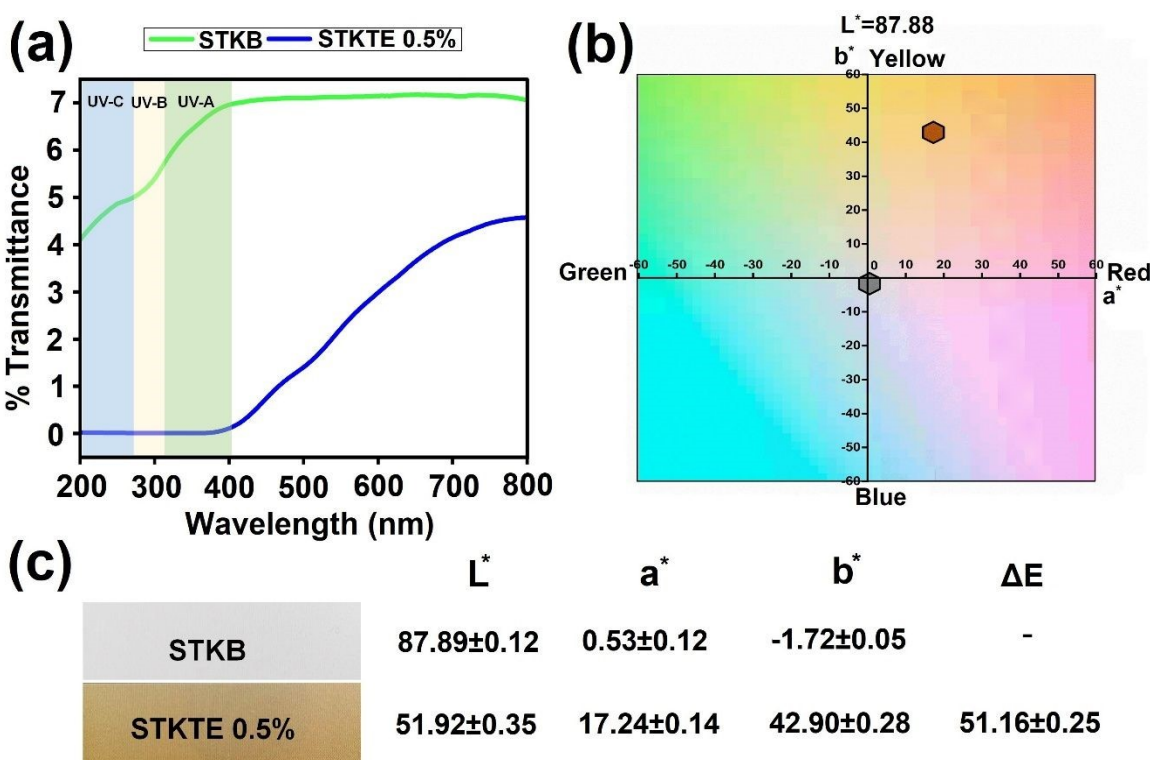


Figure 4



772

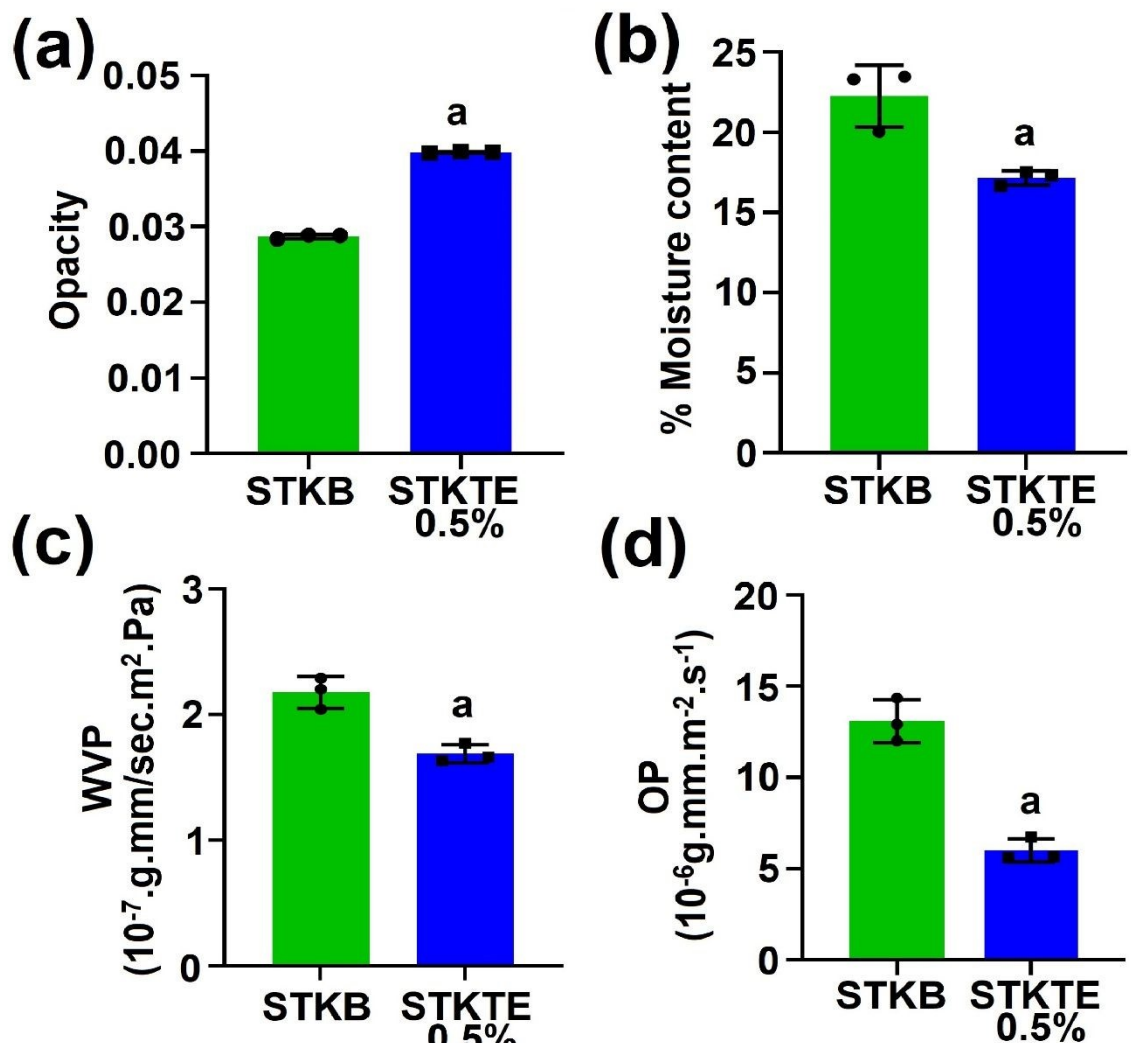
View Article Online  
DOI: 10.1039/D5FB00838G

Figure 5

773

774

775

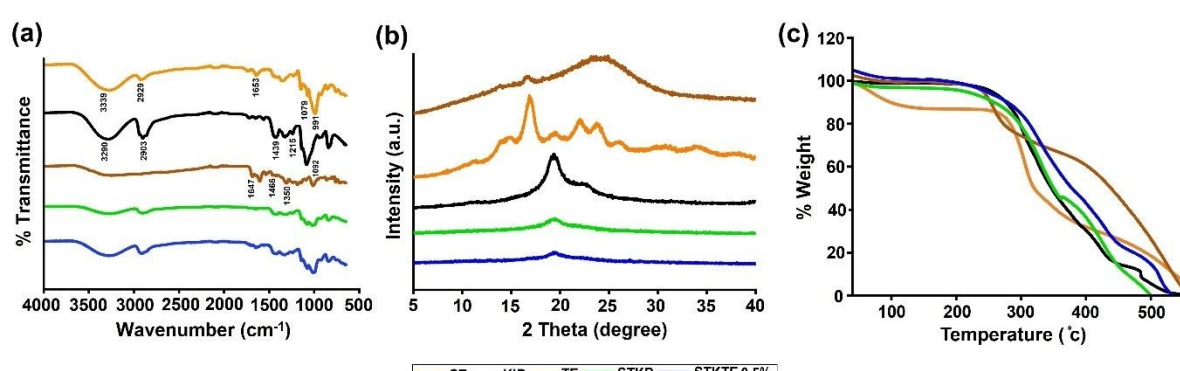


Figure 6

776

777

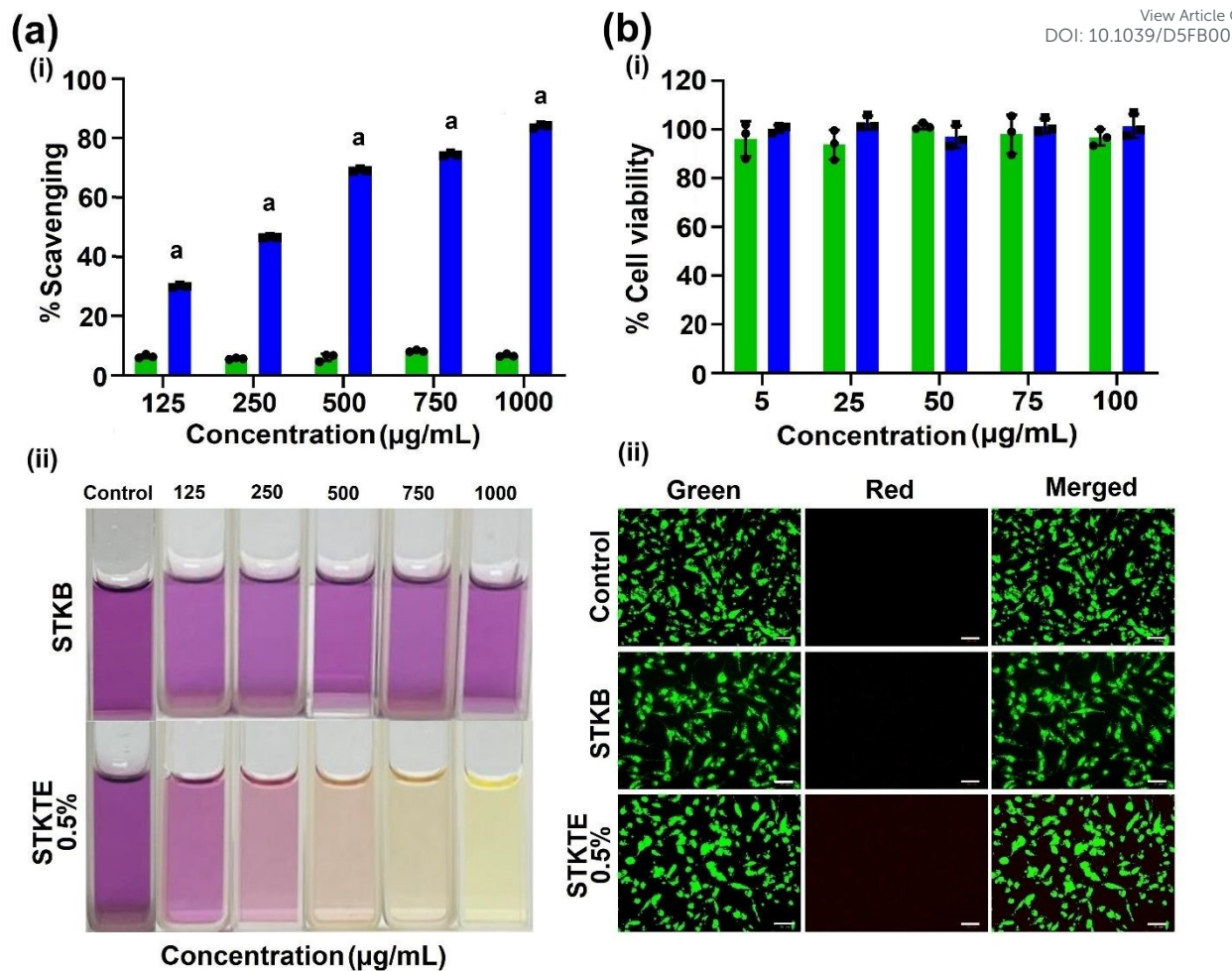


Figure 7

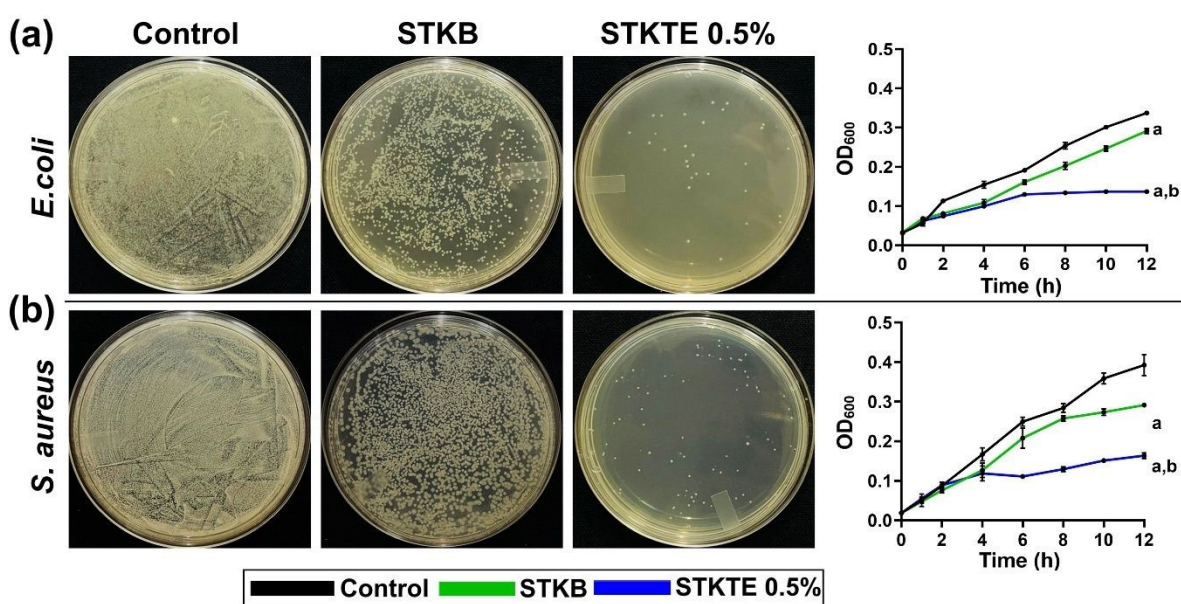


Figure 8

783

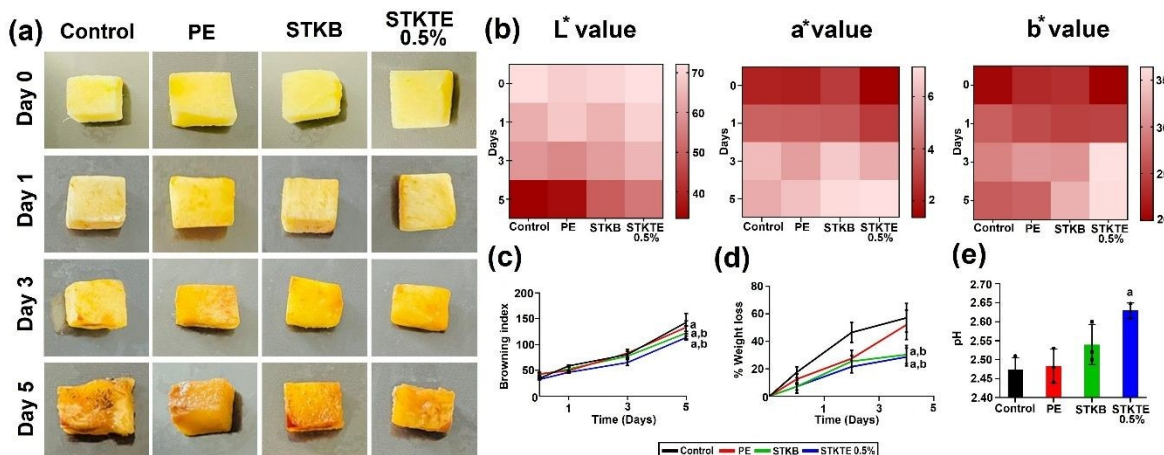


Figure 9

784

785

786

787

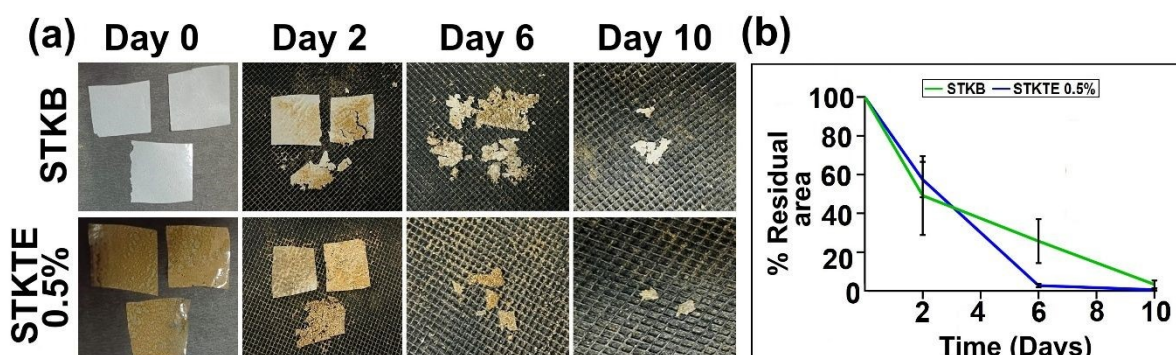


Figure 10

788

789

790

791

792

793

## Data Availability Statement

[View Article Online](#)  
DOI: 10.1039/D5FB00838G

Data supporting the findings of this study are available within the manuscript.